Interpretable machine learning for battery capacities prediction and coating parameters analysis

Kailong Liu [*], Mona Faraji Niri, Geanina Apachitei, Michael Lain, David Greenwood, James Marco

WMG, The University of Warwick, Coventry, CV4 7AL, United Kingdom
The Faraday Institution, Quad One, Harwell Science and Innovation Campus, Didcot, United Kingdom

ARTICLE INFO

ABSTRACT

Battery manufacturing plays a direct and pivotal role in determining battery performance, which, in turn, significantly affects the applications of battery-related energy storage systems. As a complicated process that involves chemical, mechanical and electrical operations, effective battery property predictions and reliable analysis of strongly-coupled battery manufacturing parameters or variables become the key but challenging issues for wider battery applications. In this paper, an interpretable machine learning framework that could effectively predict battery product properties and explain dynamic effects, as well as interactions of manufacturing parameters is proposed. Due to the data-driven nature, this framework can be easily adopted by engineers as no specific battery manufacturing mechanism knowledge is required. Reliable battery manufacturing dataset particularly for coating (one key stage) collected from a real battery manufacturing chain is adopted to evaluate the proposed framework. Illustrative results demonstrate that three types of battery capacities including cell capacity, gravimetric capacity, and volumetric capacity can be accurately predicted with R^2 over 0.98 at the battery early-manufacturing stage. Besides, information regarding how the variations of coating mass, thickness, and porosity affect these battery capacities is effectively identified, while interactions of these coating parameters can be also quantified. The developed framework makes the data-driven model become more interpretable and opens a promising way to quantify the interactions of battery manufacturing parameters and explain how the variations of these parameters affect final battery properties. This could assist engineers to obtain critical insights to understand the underlying complicated battery material and manufacturing behavior, further benefiting smart control of battery manufacturing.

1. Introduction

1.1. Literature review

Due to the superiorities in terms of high energy density and low discharge rate, lithium-ion (Li-ion) batteries have been widely viewed as a promising energy storage solution for numerous sustainable applications such as smart grid and transportation electrifications (Klintberg, Zou, Fridholm, & Wik, 2019; Liu, Gao, et al., 2022; Wang, et al., 2020). However, a major limiting step for the wider applications of Li-ion battery lies in the enhancement of its manufacturing process (Liu, Wei, et al., 2022). As a significantly complicated chain, parameters involved in each stage of battery manufacturing and their related electrochemical interactions would determine final battery performance such as its capacities directly and significantly (Kwade, et al., 2018). Therefore, it is vital to well analyze parameters within the battery production chain in the pursuit of smart control for battery manufacturing.

As battery manufacturing chain consists of a number of chemical, mechanical as well as electrical operations and would generate numerous strongly-coupled parameters or variables, engineers in particular often rely on the experiment experiences, expert advice, trial and error approach to analyze or evaluate the feature parameters within their battery manufacturing chain. These approaches result in huge laborious and time consumption, slow battery product development, inaccurate quality control, and difficulty in capturing the manufactured battery performance in the early-production cases. In light of this, advanced data science solutions to effectively analyze manufacturing parameters and better quantify their interactions during battery production are urgently required.

With the rapid development of cloud platforms and machine learning technologies, data-driven methods have become a powerful and popular tool for effective battery operation management (Hu, et al., 2019; Li, et al., 2019; Wei, et al., 2018). A good deal of data-driven

solutions have been designed to estimate battery internal states (Fang, Srivas, de Callafon, & Haile, 2017; Tang, Gao, Liu, Liu, & Foley, 2021; Zhou, Stein, & Ersal, 2017), predict battery service life under cyclic (Severson, et al., 2019; Tang, et al., 2020) or calendar ageing modes (Hu, Ma, Liu, & Sun, 2022; Hu, Ma, Sun, & Liu, 2022; Liu, Peng, et al., 2022), diagnose battery faults (Dey, et al., 2016; Hu, et al., 2020; Majdzik, Akielaszek-Witczak, Seybold, Stetter, & Mrugalska, 2016), equalize cells within a pack (Feng, et al., 2020; Feng, Hu, Liu, Lin, & Liu, 2019; Ouyang, Wang, Liu, Xu, & Li, 2019), achieve efficient energy management (Shafikhani, 2021; Shang, et al., 2019) and charging control (Liu, Li, & Zhang, 2017; Liu, Zou, Li, & Wik, 2018; Pourabdollah, Egardt, Murgovski, & Grauers, 2017). In summary, through deriving proper data-driven solutions, efficient battery management could be achieved. However, these data-driven works mainly focus on improving the performance of battery products but relatively little has been done on techniques for manufacturing their internal components. As battery manufacturing especially for several key stages such as coating could also generate available data and have a more direct impact on determining the performance of the final battery, designing a reasonable data-driven method to benefit battery smarter manufacture is worthy of study.

However, compared with the field of battery management where numerous mature data-driven solutions are available, there are still limited explorations of deriving suitable machine learning strategies to benefit battery from a manufacturing perspective (Aykol, Herring, & Anapolsky, 2020; Liu, Wang, & Lai, 2022; Wanner, Weeber, Birke, & Sauer, 2019). Among limited research on battery production (e.g., parameter monitoring (Knoche, Surek, & Reinhart, 2016), variable adjustment (Schünemann, Dreger, Bockholt, & Kwade, 2016) and quality control (Günther, et al., 2020; Ju, Li, Xiao, Huang, & Biller, 2013)), designing suitable machine learning solutions to forecast key performance indicators (KPIs) of intermediate product or properties of final battery product, as well as perform sensitivity analysis of manufacturing and control parameters of interest is drawing increasing attention. For instance, according to the cross-industry standard process (CRISP), linear as well as neural network models have been designed in Schnell, et al. (2019) for the manufacturing process dependency identification and battery manufacturing properties prediction. Turetskyy, et al. (2020) utilized the decision tree techniques to perform battery maximum capacity predictions and analyze feature importance analysis. In Turetskyy, Wessel, Herrmann, and Thiede (2021), a multi-output method through using data-driven models is proposed to predict the final product properties from intermediate manufacturing feature variables for battery manufacturing design. Duquesnoy, Lombardo, Chouchane, Primo, and Franco (2020) proposed a data-driven method named sure-independent-screening and sparsifying-operator (SISSO) to analyze the effects of uncalendared electrode structure on battery cell performance after calendering. After performing data driven-based statistical analysis of fluctuation from battery manufacturing, the fluctuation effects on the battery product capacity are explored in Hoffmann, et al. (2020). Based upon the two-dimensional graphs generated from three conventional data-driven models, the interdependencies between slurries features and battery electrode properties are analyzed in Cunha, Lombardo, Primo, and Franco (2020). After deriving a random forests-based classification framework with out-of-bag prediction, Gini index, and predictive measure of association, the importance and correlations of four parameters from mixing and coating stages within the battery manufacturing chain are analyzed in Liu, et al. (2021).

1.2. Gap analysis and original contributions

Despite the aforementioned research that gives the promising results of exploring data-driven strategies to analyze and forecast battery properties from a manufacturing perspective, there are still many limitations and challenges that need to be improved particularly for the interpretability of battery manufacturing analysis as: (1) most of the works that simply adopt the conventional machine learning methods such as neural network and support vector machine can just provide the single property prediction of battery products, lack of sensitivity analysis of relevant manufacturing or control parameters for engineers to better understand their manufacturing chain. (2) although a few machine learning tools such as tree-based techniques have been adopted to quantify feature importance and correlations of interested manufacturing parameters recently, their interpretability is still limited and worthy of further improvement. For example, random forests (RF) are a typical tree-based ensemble machine learning technique. After combining multiple individual decision trees (DTs) based on the 'bagging' solution, the final output of RF becomes the average of outputs from all DTs for the regression task (Liaw & Wiener, 2002). Through aggregating the Gini or entropy indexes of individual DTs at the forest level (Mishra & Subbarao, 2021), RF have the capability to directly quantify the importance value of all input battery manufacturing variables. To the best knowledge, limited data-driven studies are conducted to (1) explain how the variation of battery material or manufacturing parameters would dynamically affect the properties of intermediate or final battery products. (2) identify and rank the strength of interactions of interested battery manufacturing or control parameters when using them to predict battery properties. In real battery manufacturing applications, engineers are interested in understanding how the parameters of interest are interacted with each other and would specifically affect the relevant battery products' properties. Lack of these explanations would not only significantly prevent the use of data-driven models in such sensitivity analysis assessment, but also lose the opportunities to explore more in-depth underlying mechanisms of parameter dependence during battery manufacturing.

To address these research limitations, this study proposes an interpretable machine learning-based framework to predict various types of battery capacities at the early production stage, while the interactions of multiple coating parameters of interest and how the variations of these parameters would affect battery capacities are also taken into account. Some contributions of this study can be summarized as follows: (1) After identifying three important coating property parameters from a real battery manufacturing chain, an enhanced random forests-based interpretable machine learning framework is derived to predict different capacity types of battery products at the early manufacturing stage efficiently. (2) Through integrating two interpretable solutions including the accumulated local effect (ALE) and H-statistic, dynamical information regarding how the variations of coating mass, thickness, and porosity affect the relevant battery capacities is identified, while the interactions of these coating parameters can be also quantified and understood by the designed framework. (3) The prediction results as well as the complicated non-linear behavior underlying the battery manufacturing chain are comprehensively evaluated and visually interpreted for three key and different battery capacity cases (cell capacity, gravimetric capacity, and volumetric capacity). This is the first known application of improving the interpretability of RF with ALE and H-statistic tools to quantify the interactions of coating property parameters and explain how the variations of these parameters affect the capacities of relevant battery products. It is an illustration of developing effective control engineering tool to handle a key but challenging issue for industrial practitioners. Due to the superiority in terms of model interpretability and data-driven nature, the proposed framework could directly explain the dynamic effects of interested battery material parameters or intermediate manufacturing properties as well as their interactions, further helping the engineers perform experimental designs that could bring additional critical insights, eventually leading to the closed-form adjustment, control or optimization strategies for battery smarter manufacturing.
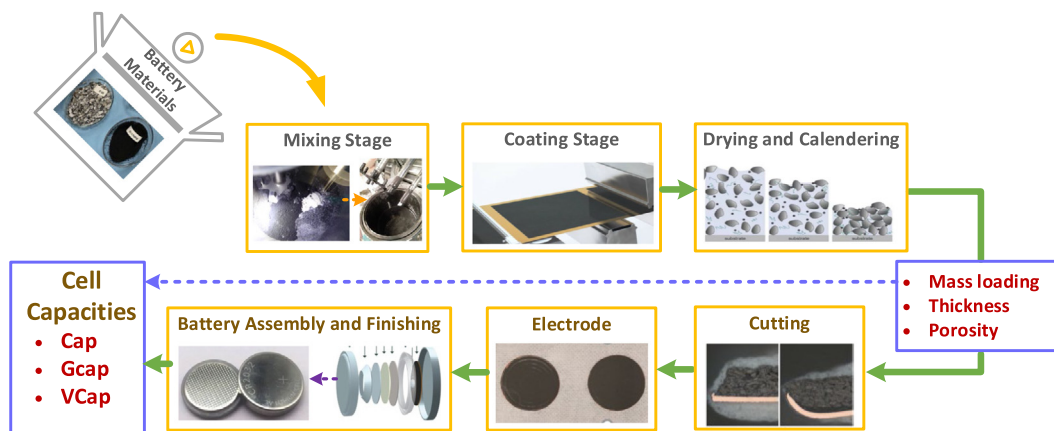
Fig. 1. Key stages of battery manufacturing particularly for electrode manufacturing.

1.3. Paper organization

The remainder of this article is organized as follows. The fundamental of the battery production chain particularly for electrode manufacturing is presented in Section 2. Section 3 details the relevant methodologies and machine learning framework to perform interpretable analysis of interested coating parameters as well as predict battery capacities. Section 4 gives the in-depth evaluation of prediction results of different battery capacities and discusses the analysis results obtained from the designed interpretable machine learning framework. Finally, the conclusion of this study is summarized in Section 5.

2. Experimental battery manufacturing

As a complex process involving numerous chemical, mechanical and electrical operations, battery manufacturing line generally consists of three primary parts including battery electrode manufacturing, battery assembly as well as battery formation (Duffner, et al., 2021). As an early production stage, battery electrode manufacturing plays a pivotal role in determining electrode property, further significantly affecting the following stages and final battery product performance (Liu, Hu, Meng, Guerrero, & Teodorescu, 2021).

Fig. 1 summarizes several key and individual battery manufacturing stages especially for battery electrode production. Specifically, after preparing suitable materials such as active materials (NMC-622 and graphite), conductive additives (carbon black), solvent (N-Methyl-2-pyrrolidone or water) as well as binder, Li-ion battery electrode manufacturing would usually start with a mixing stage to mix these materials within a mixing tank such as soft blender. Then the generated slurries from the mixing stage will be coated onto the surface of metal foils during a coating stage. For anode and cathode electrodes, the slurries would be generally coated onto the surface of copper foil and aluminum foil, respectively (Reynolds, Slater, Hare, Simmons, & Kendrick, 2021). After that, the coating products would be dried by a dryer such as an oven with predefined temperatures and then move to the calendering stage for evaporating the residual solvent. Finally, a cutting or slitting stage would be conducted to cut the calendered electrode into suitable sizes. It should be known that numerous highly-nonlinear manufacturing parameters and strongly coupled intermediate product variables could be generated during battery electrode production line (Liu, Wei, et al., 2022). In light of this, manufacturing parameters and intermediate product properties within battery electrode production must be well monitored and analyzed.

In this context, to enable the training and evaluation activities of the interpretable machine learning framework, a real battery scale-up manufacturing line in the Warwick manufacturing group (WMG) is set up to generate available battery manufacturing data particularly for the coating stage. The parameters of this battery manufacturing line would

be changed in a systematic manner to affect electrode structure, further producing cathode coating with different physical properties of mass loading (mass), thickness, and porosity. For this study, the electrode active material is the nickel manganese cobalt oxide that formed 96% of the whole cathode slurry mixture. The mixture also contains 2% of additive carbon black, and 2% of polyvinylidene fluoride binder. Coating stage is performed via the lab-scale coating machine of Dürr Megtec, as shown in Fig. 2(a). This machine uses the comma bar technology to generate shear force and equips with a 3-zone thermal dryer to generate an effective drying length of almost 4 m. Fig. 2(b) details the comma bar equipment to deposit the slurry onto the electrode foil, while the oven and dryer would be then used to evaporate the slurry solvent and provide the final electrode product. During battery electrode manufacturing process, the slurry would be first prepared within a mixing tank, as illustrated in Fig. 2(c). Then the prepared slurry will be continuously checked to ensure the desired quality. After the comma bar coating stage, the slurry would be deposited onto the surface of aluminum foil with a thickness of 15um. Fig. 2(d) shows a case of the coated foil.

After that, the battery electrode product would be cut into several disks with a diameter of 15 mm. These disks will be then adopted to assemble battery coin cells in 2032 size. It should be known that this battery assembly process is conducted manually within the isolated rooms. As this study focuses on the cathode electrode, the counter electrode is Li-metal to minimize the effects of anode uncertainties on the sensitivity analysis studies and predictability of the derived data-driven model.

To obtain useful battery manufacturing dataset for battery capacities prediction and coating parameters analysis, some feature parameters including the coating mass loading (mass), coating thickness and electrode weight require to be measured. Specifically, the coating mass is measured by a high precision scale for weight with an error below 0.0001 grams. Coating thickness is measured by a high-quality micrometre with accuracy in micrometre range. Based on these two feature parameters, coating porosity of the cells could be then obtained as a dimensionless number in percent (%) by:

$$porosity = 1 - \frac{gsm}{\rho_{avg} * th} \tag{1}$$

where gsm denotes the coating mass loading with the unit of g/m^2; th shows the coating thickness with the unit of um; ρ_{avg} stands for the average density of the coating with the unit of g/cm^3.

Following this process, 115 battery coin-cells are produced in the battery manufacturing line. These battery cells would then go to a testing stage for extracting their electrochemical properties such as capacities. Specifically, the cells are placed in a thermal chamber with an ambient temperature of 25 °C and would be cycled with constant-current constant-voltage (CCCV) charging and constant-current (CC)
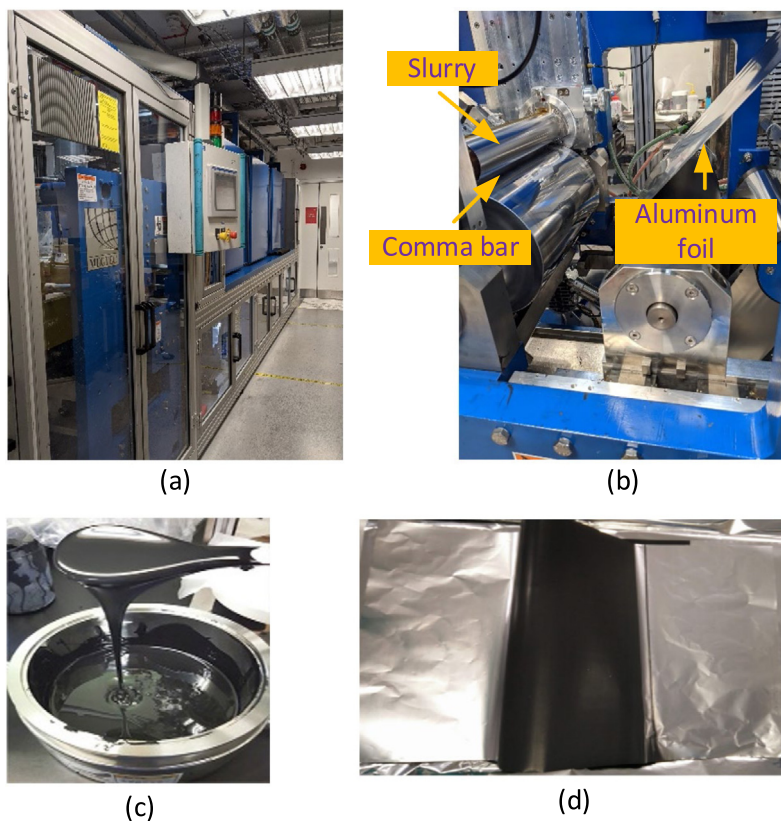
Fig. 2. Battery scale-up manufacturing line in WMG to produce battery electrode: (a) laboratory scale electrode manufacturing machine, (b) comma bar coating machine, (c) cathode slurry mixture, (d) coated foil.

discharging. Then battery cell capacity (Cap) with the unit of mAh would be obtained after fully discharging each cell from its up cut-off voltage to down cut-off voltage as an index for Cap. According to the measured cell weight and dimension, another two types of capacities including the gravimetric capacity (GCap) with unit of mAh/g as well as the volumetric capacity (VCap) with unit of mAh/cm^3 can be obtained as:

$$\begin{cases} GCap = Cap/weight \\ VCap = Cap/volume \end{cases} \tag{2}$$

where $weight$ represents the weight of a single cell with the unit of g; $volume$ means the cell coating volume with the unit of cm^3 that can be obtained by multiplying coating area ($area$) and th as:

$$volume = area \times th \tag{3}$$

Based on the above-mentioned progress, the dataset that contains three coating parameters (mass, thickness and porosity) and three various types of capacities (Cap, GCap and VCap) can be generated and collected. Then the interpretable machine learning framework could be established after preprocessing this experimental battery manufacturing dataset.

3. Methodology

This section details the machine learning-based methodology and framework to achieve a reliable interpretation for the effects of coating parameters on various types of battery capacities. Specifically, the random forests-based regression model is first introduced, followed by the descriptions of accumulated local effects as well as H-statistic tool for feature dynamic effects analysis and feature interaction quantification, respectively. Furthermore, the framework designed in this study to predict battery three different types of capacities and analyze related coating parameters is derived.

3.1. Random forests

Due to the merits of non-parametric behavior and simplification, classification and regression tree (CART) is generally utilized as the DT within RF (Loh, 2011). The detailed structure of RF regression is shown in Fig. 3.

For the RF-based regression, supposing training set $TS = \{(X_1, Y_1), (X_2, Y_2), \ldots, (X_m, Y_m)\}$ contains m observations, each input vector $X_i = (X_{i1}, X_{i2}, \ldots, X_{iN})$ has N features, while Y_i is the output of RF. The work flow to establish a RF-based regression model is detailed in Table 1 as follows:

The key step of RF-based regression model training is to construct individual DTs. Through using the specific bootstrap samples to train each DT, the diversity of DT could be significantly increased. Furthermore, the correlations of DTs are effectively reduced. That is, RF could be established without pruning, leading to a relatively low computational effort. Through averaging numerous de-correlated DTs to obtain prediction results, RF could become less sensitive to the noise. For the construction of each DT, based upon the bagging solution, not all TS will be selected as the bootstrap sample. This could result in some observations named the out-of-bag (OOB) samples would not be adopted for training a DT. In general, the number of OOB samples reaches nearly one-third of TS. After a DT is established, its OOB samples could be utilized to achieve an unbiased estimation. In this way, the over-fitting issue can be relieved, further enhancing the generalization performance of RF.

3.2. Accumulated local effects

In the previous work (Liu, et al., 2021), a flexible RF-based model is established to predict the battery electrode properties and quantify the importance as well as correlations of four manufacturing variables of interest. The results illustrate the superiorities of RF in model-
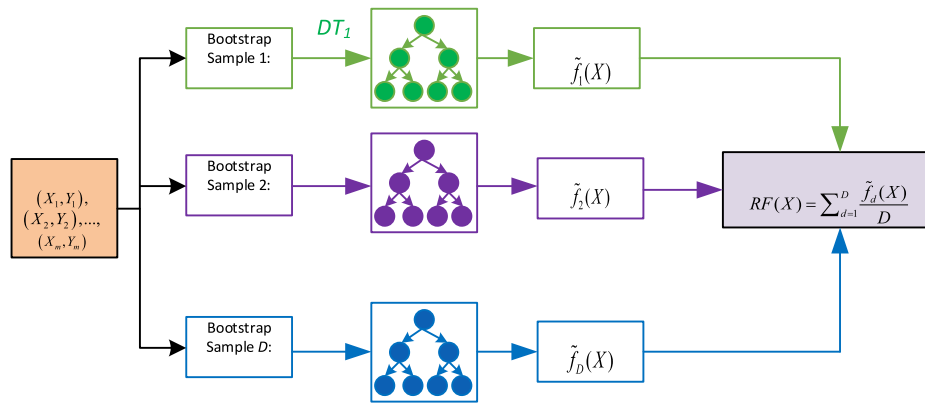
Fig. 3. Structure of RF-based regression model.

Table 1
Detailed flow to establish a RF-based regression model for predicting battery capacities.

1: **Procedure:** RF-based regression model training

2:     For $d = 1$ to D: (D is the number of DTs)

3:     Formulating the bootstrap sample BS_d with M observations from training set TS

4:     Training the tree DT_j based on the related BS_d

    (a). Splitting a node based on all the observations of BS_d

    (b). For all unsplit nodes, repeating the following procedures recursively:

    (i). Selecting n features from N features pool randomly: $n \leftarrow N(n < N)$

    (ii). Discovering a split way that could provide the best impurity among all splits of n features from step (i).

    (iii). Splitting this node into two sub-nodes through using the discovered split way from step (ii).

5:     Constructing the RF regression model by ensembling all trained tree learners $f_d(\cdot) : d = 1 : D$.

6: **End procedure**

7: **Procedure:** RF-based regression model prediction

8: After constructing the RF-based regression model $RF(\cdot)$, its output $RF(X)$ for a new observation X as input can be obtained by:

$$RF(X) = \sum_{d=1}^{D} \frac{f_d(X)}{D}$$

where $f_d(X)$ reflects the prediction results of all well-trained DTs with a total number of D.

9: **End procedure**

ing and analyzing feature variables within the battery manufacturing chain. However, it is difficult for the traditional RF model to explain prediction mechanisms such as how the features would dynamically affect the prediction results. In many applications, understanding the prediction mechanism of an established model is much more conducive to the application of model. Besides, it could also benefit the battery manufacturer to analyze how manufacturing parameters specifically affect the performance of relevant battery products. In this study, to obtain information regarding how the variation of coating parameters would dynamically affect battery capacities, the accumulated local effect (ALE) is explored based on the well-established RF model.

In theory, ALE is able to explain how feature parameters of interest would affect the prediction of a model on average. The key of ALE is to simplify a complicated prediction function f to a function that only relies on several factors. Then the ALE plots are capable of averaging the variations of predictions and accumulating them over the grid. To quantify local effects, features would be divided into many intervals and the uncentered effect would be estimated by:

$$\widehat{\tilde{f}}_{j,ALE}(x) = \sum_{k=1}^{k_j(x)} \frac{1}{n_j(k)} \sum_{i:\, x_j^i \in N_j(k)} [f(z_{k,j}, x_{\setminus j}^{(i)}) - f(z_{k-1}, x_{\setminus j}^{(i)})] \quad (4)$$

where $z_{k,j}$ represents the boundary value of the kth interval for the jth feature, $n_j(k)$ stands for the amount of samples in the kth interval, $i : x_j^i \in N_j(k)$ means the ith sample point in the kth interval, $x_{\setminus j}$ stands

for the features other than feature j. In order to make the mean effect becomes zero, this ALE estimator can be centered by:

$$\hat{f}_{j,ALE}(x) = \widehat{\tilde{f}}_{j,ALE}(x) - \frac{1}{n} \sum_{i=1}^{n} \widehat{\tilde{f}}_{j,ALE}\left(x_j^{(i)}\right) \quad (5)$$

The value of $\hat{f}_{j,ALE}(x)$ could be interpreted as the main effect of the jth feature at a certain point in comparison with the average prediction of the data. It should be known that ALE plots are able to not only present the effect of single feature parameter, but also could reflect the interaction effect of two feature parameters. In this context, the main and overall mean effects of two feature parameters of interest would be adjusted. Specifically, the ALE plots for two feature parameter cases would only reflect the second order effects (the additional interaction effects) of these two feature parameters rather than their main effects (Molnar, 2020). To calculate the ALE-based second-order effect of feature pair x_j and x_l, the sample ranges of ALE plots would be divided into K^2 rectangular cells. Supposing k and m stand for the indices into the grid corresponding to x_j as well as x_l respectively, the uncentered effect of these feature pair can be calculated by:

$$\hat{h}_{\{j,l\},ALE}(x_j, x_l) = \sum_{k=1}^{k_j(x_j)} \sum_{m=1}^{k_l(x_l)} \frac{1}{n\{j,l\}(k,m)}$$

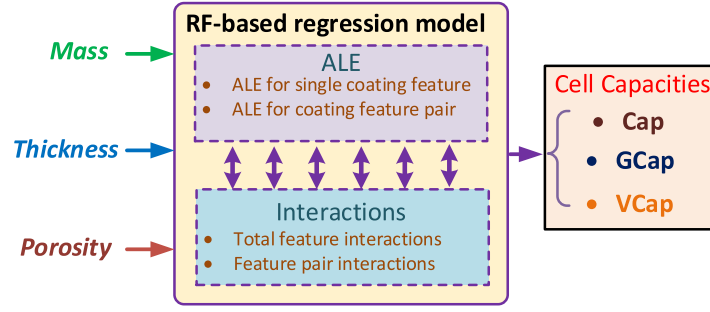$$\times \sum_{i:\, x_{\{j,l\}}^{(i)} \in N_{\{j,l\}}(k,m)} \triangle_f^{\{j,l\}}\left(K, k, m; x_{\{j,l\}}^{(i)}\right) \quad (6)$$

Fig. 4. The structure of RF-based regression model with interpretability.

where $\triangle_f^{\{j,l\}}\left(K,k,m;x_{\{j,l\}}^{(i)}\right)$ represents the second-order finite difference of $f\left(x_i,x_l,x_{\{j,l\}}^{(i)}\right)$ for (x_i,x_l) across cell $(x_{k-1,j},x_{k,j})\times(x_{m-1,l},x_{m,l})$. Then, the ALE second-order effect $\widehat{\widetilde{f}}_{\{j,l\},ALE}\left(x_j,x_l\right)$ of x_j and x_l pair could be calculated as:

$$\widehat{\widetilde{f}}_{\{j,l\},ALE}\left(x_j,x_l\right)=\hat{h}_{\{j,l\},ALE}\left(x_j,x_l\right)$$
$$-\sum_{k=1}^{k_j(x_j)}\frac{1}{n_j(k)}\sum_{m=1}^{k}n_{\{j,l\}}(k,m)\left\{\hat{h}_{\{j,l\},ALE}\left(x_{k,j},x_{m,l}\right)\right.$$
$$-\hat{h}_{\{j,l\},ALE}\left(x_{k-1,j},x_{m,l}\right)\}$$
$$-\sum_{m=1}^{k_l(x_l)}\frac{1}{n_l(m)}\sum_{k=1}^{k}n_{\{j,l\}}(k,m)\left\{\hat{h}_{\{j,l\},ALE}\left(x_{k,j},x_{m,l}\right)\right.$$
$$-\hat{h}_{\{j,l\},ALE}\left(x_{k,j},x_{m-1,l}\right)\} \tag{7}$$

Finally, this ALE second-order effect could be centered by Apley and Zhu (2020):

$$\hat{f}_{\{j,l\},ALE}\left(x_j,x_l\right)=\widehat{\widetilde{f}}_{\{j,l\},ALE}\left(x_j,x_l\right)$$
$$-\frac{1}{n}\sum_{k=1}^{K}\sum_{m=1}^{K}n_{\{j,l\}}(k,m)\widehat{\widetilde{f}}_{\{j,l\},ALE}\left(x_{k,j},x_{m,l}\right) \tag{8}$$

3.3. Feature interaction

As the feature parameters within battery manufacturing chain present interactivity, the influence of these parameters on the manufactured battery properties would become not simply cumulative, but more complex. After well-establishing the RF-based regression model, an effective solution named H-statistic could be derived to analyze and quantify the strength of feature interaction (Kern, 2020). Mathematically, the interaction between the jth feature and the kth feature through using the H-statistic tool can be calculated by:

$$H_{jk}^2=\sum_{i=1}^{n}[PD_{jk}\left(x_j^{(i)},x_k^{(i)}\right)-PD_j\left(x_j^{(i)}\right)-PD_k\left(x_k^{(i)}\right)]^2/\sum_{i=1}^{n}PD_{jk}^2(x_j^{(i)},x_k^{(i)}) \tag{9}$$

where PD_{jk} represents the two-way partial dependence function (PDF) of the jth and the kth features. Here $PD_{jk}\left(x_j,x_k\right)=PD_j\left(x_j\right)+PD_k\left(x_k\right)$, and PD_j as well as PD_k are PDFs of the jth feature and the kth feature, respectively. Then the H-statistic of jth feature interacting with any other features can be calculated by:

$$H_j^2=\sum_{i=1}^{n}[\hat{f}\left(x^{(i)}\right)-PD_j\left(x_j^{(i)}\right)-PD_{-j}\left(x_{-j}^{(i)}\right)]^2/\sum_{i=1}^{n}\hat{f}^2\left(x^{(i)}\right) \tag{10}$$

where the prediction function $\hat{f}(x)$ represents the function that sums all PDFs, $PD_{-j}\left(x_{-j}\right)$ stands for the PDF relying on all other features except the jth feature.

3.4. Designed interpretable machine learning framework

For a battery cell, its capacities would be highly affected by its coating properties within a production chain. To well predict the cell capacities and effectively analyze the coating feature parameters through using interpretable machine learning, an RF-based regression model structure with enhanced interpretability is derived, as shown in Fig. 4. Specifically, the inputs of this model structure are three coating property parameters of interest including the coating mass (g/m^2), coating thickness (um) and coating porosity (%), while three different cell capacities including the cell capacity (Cap) with the unit of mAh, gravimetric capacity (GCap) with the unit of mAh/g, and the volumetric capacity (VCap) with the unit of mAh/cm^3 are utilized as the output of the model structure, respectively. Besides, through combining the powerful interpretable tools including ALE and H-statistic, how coating features affect the predicted capacity results and the level of feature interaction among these three coating parameters can be also obtained. In this study, to independently explore how the variation of coating parameters would dynamically affect the predictions of three different battery capacity types, three different RF models are trained to individually predict each of the three outputs. The detailed framework through designing the RF-based interpretable framework to predict three various cell capacities and analyze how these three coating parameters affect the produced cell capacities is illustrated in Fig. 5. This framework mainly contains four parts and can be summarized as follows

(1) **Data curation and preprocess:** after collecting battery coating parameters data and related battery performance data, a data curation and preprocess step is carried out. Specifically, the obvious outliers from data and the vectors that own the missing data points are first removed. Then the suitable data matrix that could well reflect the inputs and output pair of the RF-based regression model (as illustrated in Fig. 4) will be constructed. In this study, model inputs are always the three coating property parameters of interest (mass, thickness and porosity). The samples of Cap, GCap and VCap corresponding to these coating parameters are respectively selected as the model output, finally formulating three data matrices for model training and parameter analysis.

(2) **RF-based regression model construction:** after constructing suitable input–output matrices, RF-based regression model can be trained to capture the underlying mappings among inputs–output observations by following the steps from Workflow 1. It should be known that the RF model is user-friendly with only a few hyperparameters need to be set. These hyperparameters include the number of DTs (D) and the number of features for each node split (n). In theory, more DTs would increase the prediction accuracy and generalization of RF, but too many DTs will also inevitably increase RF's computational burden. For the number of features to split node within a DT, a larger n would benefit the strength of each DT but also results in the correlations of DTs increase. According to Biau and Scornet (2016), $D = 100$ is enough for the small-scale observations like this case, while setting $n = 2N/3 = 2$ is a recommended choice for the regression applications.
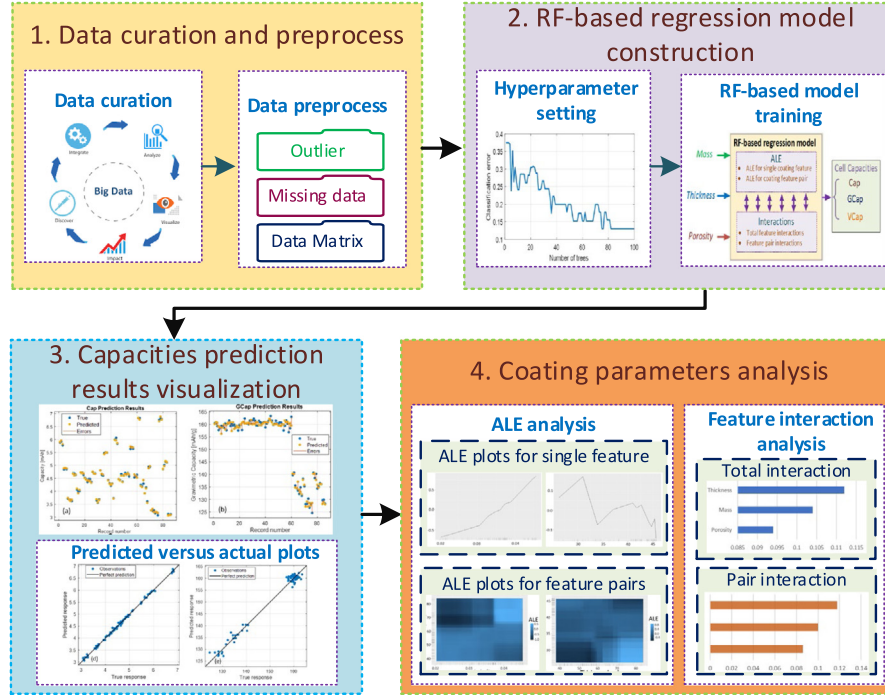
Fig. 5. Detailed interpretable ML framework through using RF-based regression model to predict cell capacities and analyze coating parameters.

(3) **Capacities prediction results visualization:** after well establishing the RF-based regression model, three types of cell capacities (Cap, GCap, VCap) would be predicted for new coating parameter observations. Then the cell capacities prediction results can be visualized through using effective tool such as scatter plot and predicted versus actual plot. To well quantify the prediction performance of designed RF-based model, performance indicators should be adopted. Supposing M is the total number of observations, y_i and $\tilde{y}_i$ represent the real capacities and the predicted capacities respectively (here $i = 1, 2, \ldots, M$), $\overline{y}$ is the mean value of all response capacities, then three widely-used indicators including the maximum absolute error (MAE), the root mean square error (RMSE) and the R^2 value (Niri, et al., 2021) are adopted to evaluate the capacity prediction results in this study and can be calculated as follows:

$$\begin{cases} MAE = \frac{max}{1 \le i \le M} |y_i - \tilde{y}_i| \\ RMSE = \sqrt{\frac{\sum_{i=1}^{M}(y_i - \tilde{y}_i)^2}{M}} \\ R^2 = 1 - \sum_{i=1}^{M}(y_i - \tilde{y}_i)^2 / \sum_{i=1}^{M}(y_i - \overline{y})^2 \end{cases} \quad (11)$$

Obviously, MAE could reflect the maximum absolute difference between the prediction results and the real capacity values, while RMSE and R^2 value are able to reflect the overall prediction performance. The larger the MAE, the bigger the prediction deviation is. The smaller the RMSE, the better the prediction accuracy is. The R^2 would get close to 1 when the prediction capacities are close to the real test values.

(4) **Coating parameters analysis:** in this part, to analyze coating feature parameters of interest, two interpretable machine learning tools are designed based on the well-trained RF regression model. Specifically, the ALE plots are given to explain how coating parameters affect the produced cell capacities, while H-statistic is used to quantify the feature interactions of these coating parameters. According to Eqs. (5) and (8), the values of ALE for both single coating feature parameters (mass, thickness, porosity) and corresponding feature pairs can be obtained, respectively. Then the 2D ALE plots and ALE matrix plots can be visualized to reflect how single coating feature and coating feature pairs affect the predicted capacity values of produced cell. For the

feature interactions, according to Eqs. (9) and (10), two types of feature interaction including the total interaction of each coating parameter and the interaction of corresponding coating parameter pairs can be quantified respectively. In theory, larger interaction values indicate there exist stronger interactions between the coating parameter pairs of interest.

Following these steps, a flexible interpretable machine learning framework based on the RF regression model can be built to not only well predict various types of battery cell capacities, but also quantify the feature interactions of interested coating parameters as well as explain how these parameters dynamically affect the produced cell capacities. In this way, more information especially for how coating parameters specifically affect battery performance could be explored in-depth.

4. Results and discussions

In this section, to predict cell capacities, analyze how coating parameters dynamically affect the capacity results, and quantify the related feature interaction, the designed interpretable machine learning framework is first adopted to predict three various types of cell capacities, followed by the detailed analysis of dynamic effects and interaction of involved coating parameters.

4.1. Capacities prediction results

According to the structure as illustrated in Fig. 4, three coating parameters including coating mass, coating thickness, and coating porosity are utilized as inputs, while three different battery capacities (Cap, GCap, and VCap) are utilized as the output of derived model, respectively. To evaluate the prediction performance of RF-based regression models, all three capacity prediction cases are carried out by using the five fold cross-validation. Fig. 6 and Table 2 show the battery cell capacities prediction results and related performance indicators, respectively.

From the prediction results of Cap case in Fig. 6(a), it is evident that nearly all real observations match well with the predicted outputs from relevant RF-based regression model. Besides, according to its predicted
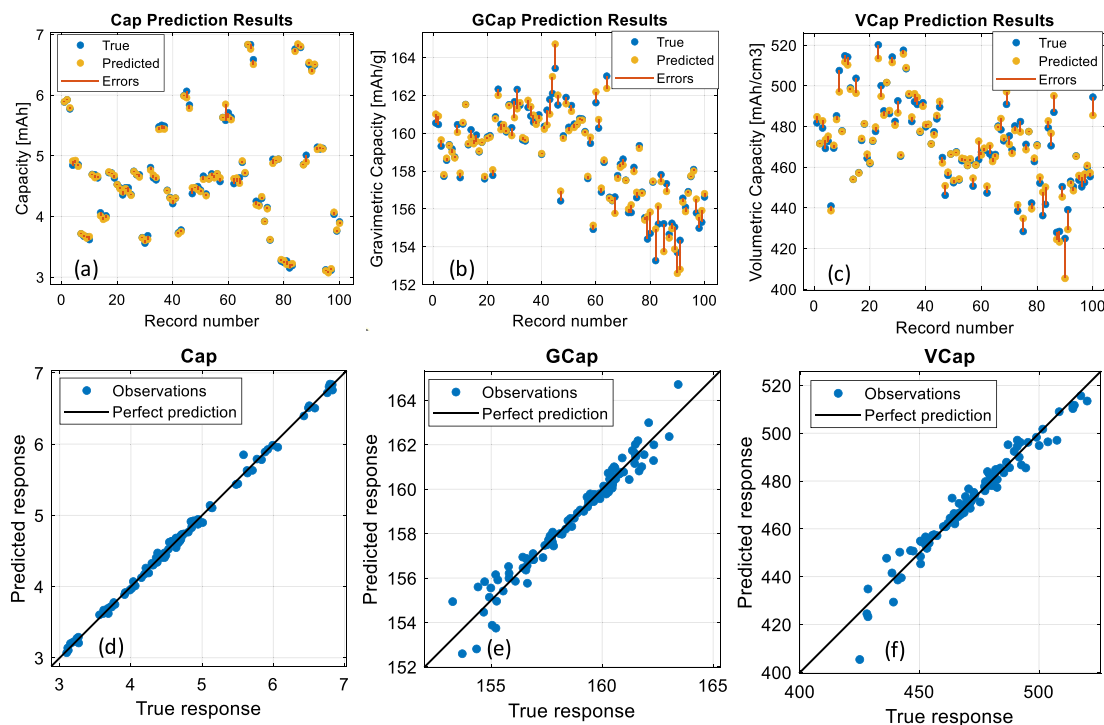
Fig. 6. Capacities prediction results. (a): Cap case, (b): GCap case, (c): VCap case, (d): Predicted versus actual plots for Cap, (e): Predicted versus actual plots for GCap, (f): Predicted versus actual plots for VCap.

Table 2
Prediction performance indicators for three battery capacity types through using derived regression models.

Capacity types	Cap [mAh]	GCap [mAh/g]	VCap [mAh/cm^3]
MAE	0.036	1.412	16.912
RMSE	0.046	1.539	4.820
R^2	0.998	0.994	0.98

versus actual plots (PVAPs) in Fig. 6(d), all observations well cluster around the perfect prediction line with the MAE of only 0.036 mAh. All these results can indicate that using three coating parameters (mass, thickness, porosity) could well determine the cell capacity values. For GCap and VCap, according to Fig. 6(b) and Fig. 6(c), the prediction results become worse as the difference between the predicted observations and real observations increases for both these two prediction cases. This is reasonable as GCap involves new element of *weight* while VCap involves new element of *volume*. However, according to Fig. 6(e) and Fig. 6(f), all the predicted observations are still clustered around their perfect prediction lines without large outliers. Based upon the results of five fold cross-validation, the corresponding R^2 values of all battery capacity cases are larger than 0.98. These indicate that through inputting these three coating parameters into the proposed RF-based models, satisfactory accuracy and generalization capabilities could be obtained for the early-stage prediction cases of all these types of battery capacity.

4.2. Capacity case study

After predicting all types of battery energy capacity based on the RF regression model, the explanation of how the interested coating parameters affect these predictions is then carried out. For the battery capacity (Cap) case, the related ALE plots to reflect how single feature (mass, thickness, and porosity) as well as feature pair (mass-thickness, mass-porosity, and thickness-porosity) affect battery Cap prediction performance are illustrated in Fig. 7.

From Fig. 7, all these three coating parameters present the strong effects on the cell capacity prediction. For coating mass and thickness, it is interesting to note that the ALE values of Cap present a monotonically increasing relationship with both these two cases, as illustrated in Figs. 7(a) and 7(b). That is, the larger the coating mass and thickness, the higher the cell capacity is obtained. For coating porosity, the overall probability of obtaining high values of cell capacity will be decreased as the value of coating porosity increases. Figs. 7(d), 7(e) and 7(f) illustrate the three two-dimensional ALE plots for feature pairs: mass-thickness, mass-porosity and thickness-porosity, respectively. These three subplots could reflect the second-order effects of these feature pairs on the prediction performance of cell capacity. Here, the second-order effect represents additional interaction effects of two parameters without containing their main effects. Light and dark shades indicate the above and below average predictions, respectively. For instance, Fig. 7(d) reveals the interaction effect between coating mass and coating thickness: for the coating products with higher mass and thickness, an additional positive effect on the cell capacity prediction is shown. Figs. 7(e) and 7(f) indicate that low coating mass and porosity, high coating thickness and low porosity give the additional positive effects to the battery cell capacity prediction.

Next, after using H-statistic solution, the total interactions as well as feature pair interactions for battery cell capacity case are quantified and illustrated in Fig. 8. Quantitatively, coating thickness provides the largest total interaction value, which is 7.7% larger than that of coating mass. In contrary, coating porosity shows the smallest total interaction value (nearly 16.1% less than that of coating thickness). These results are reasonable and can be explained as in this case the interaction value of thickness-mass feature pair is largest, while mass-porosity pair gives the smallest feature pair interaction value, as illustrated in Fig. 8(b). This finding signifies that among these three coating parameters, thickness has the largest interactions with other two parameters for battery cell capacity prediction. Porosity is the feature term with smallest interaction.
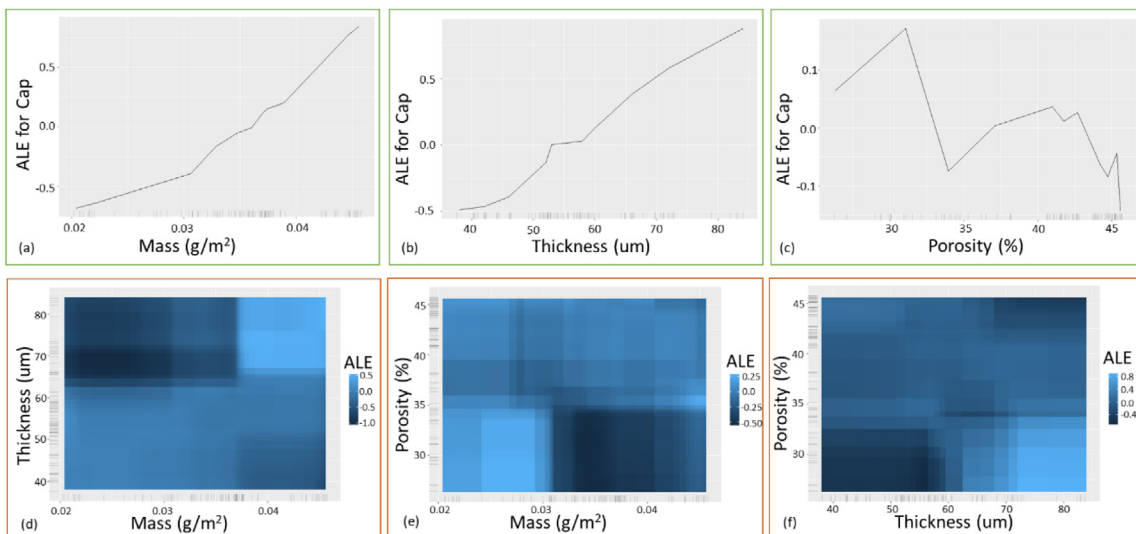
Fig. 7. ALE results for Cap case study. (a): ALE versus Mass, (b): ALE versus Thickness, (c): ALE versus Porosity, (d): Two-dimensional ALE plots for Mass and Thickness, (e): Two-dimensional ALE plots for Mass and Porosity, (f): Two-dimensional ALE plots for Thickness and Porosity.
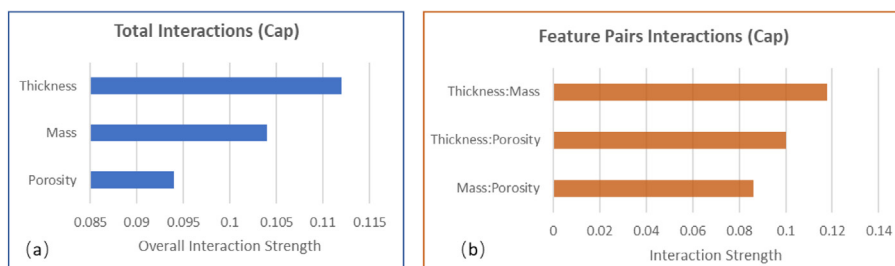

Fig. 8. Feature interactions for Cap case study. (a): Total interactions, (b): Feature pair interactions.
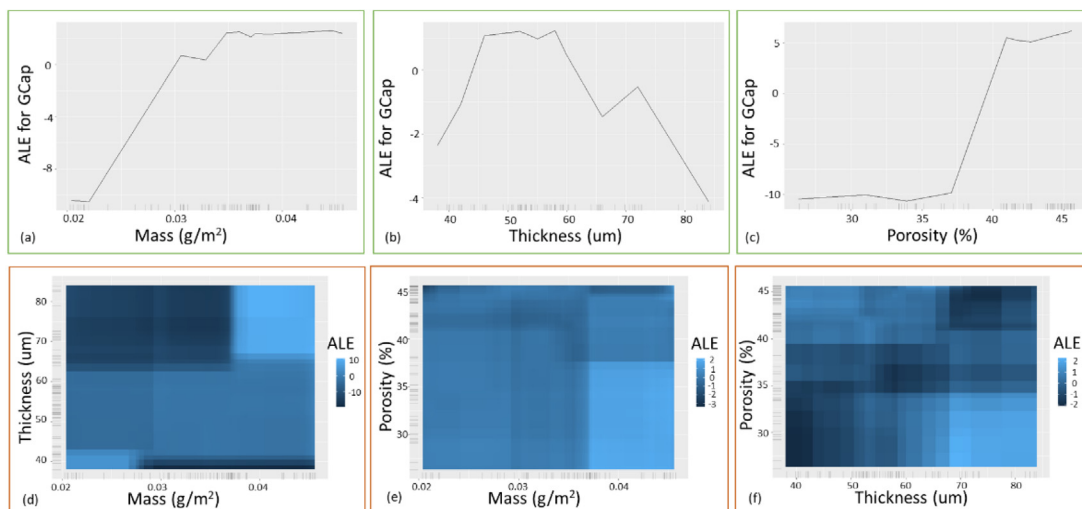

Fig. 9. ALE results for GCap case study. (a): ALE versus Mass, (b): ALE versus Thickness, (c): ALE versus Porosity, (d): Two-dimensional ALE plots for Mass and Thickness, (e): Two-dimensional ALE plots for Mass and Porosity, (f): Two-dimensional ALE plots for Thickness and Porosity.

4.3. Gravimetric capacity case study

Next, the case study of analyzing battery gravimetric capacity is carried out. Through using the designed interpretable machine learning framework, the ALE results for the dynamic effects of these three coating parameters (mass, thickness, and porosity) on the predicted probability of battery GCap are shown in Fig. 9. For coating mass, the probability of increasing battery GCap would become larger as the value of mass increases. After coating mass goes beyond 0.035 g/m^2, this probability would not change much. Coating porosity also presents a positive effect on the increase of battery gravimetric capacity. In contrary, the probability of increasing battery GCap would first increase and then keep constant as the coating thickness goes up to 58um. After this thickness point, the ALE value of GCap would present a monotonically decreasing relationship with the increase of coating thickness. According to the two-dimensional ALE plots as shown in
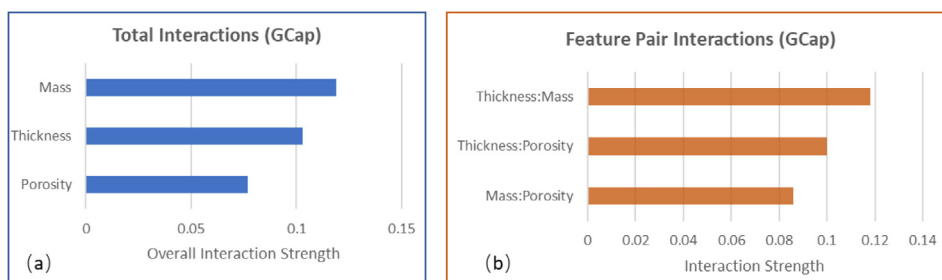
Fig. 10. Feature interactions for GCap case study. (a): Total interactions, (b): Feature pair interactions.
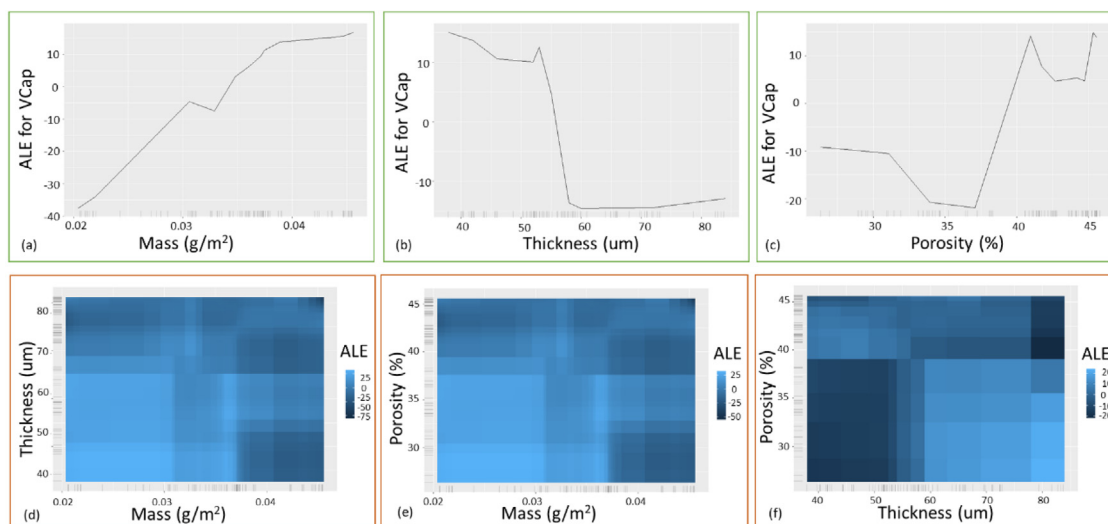

Fig. 11. ALE results for VCap case study. (a): ALE versus Mass, (b): ALE versus Thickness, (c): ALE versus Porosity, (d): Two-dimensional ALE plots for Mass and Thickness, (e): Two-dimensional ALE plots for Mass and Porosity, (f): Two-dimensional ALE plots for Thickness and Porosity.

Figs 9(d), 9(e) and 9(f), high coating mass and thickness, high coating mass and low porosity, high coating thickness and low porosity would give the additional positive effects to the battery gravimetric capacity prediction.

Fig. 10 illustrates the total interactions and feature pair interactions for the case study of battery GCap. It can be seen that the total interaction of coating mass is relatively strongest with 0.12, which is 14% and 52% larger than that from coating thickness and porosity, respectively. According to the two-way feature pair interactions in Fig. 10(b), as expected, the interactions of coating mass and thickness are larger than other pairs. This indicates that coating mass and thickness provide more interactions with other parameters for battery gravimetric capacity prediction case.

4.4. Volumetric capacity case study

Finally, the dynamic effects and interactions of three coating parameters on the battery volumetric capacity are analyzed. Fig. 11 illustrates the ALE plots estimated for coating mass, thickness and porosity on the predicted probability of battery VCap. Again, the large dynamic effects of these three coating parameters on the VCap prediction are reflected. For coating mass, the probability of increasing battery VCap becomes larger as the value of this parameter increases. Coating thickness provides a general negative effect. That is, the larger the coating thickness, the higher probability the VCap would be decreased. There exists a more complicated relation for coating porosity. Specifically, ALE value of VCap would be first reduced to −22 as the porosity value increases to 37%. After that, this ALE value would increase as coating porosity continues increasing, followed by a fluctuation during 40%–45% range. For the dynamic effects of coating parameter pairs on battery volumetric capacity, as illustrated in Figs. 11(d), 11(e) and 11(f), low coating mas and thickness, low coating mass and porosity, as well as high coating thickness but low porosity would generate larger values of two-dimensional ALE, further providing additional positive influence on the increase of battery volumetric capacity.

Then the feature interactions of all three coating parameters by using H-statistic for battery volumetric capacity case are reported in Fig. 12. Quantitatively, the interaction strength for coating thickness is relatively strongest with 0.197 (21.6% larger than that of coating mass), while coating porosity achieves the weakest interaction with other parameters with a value of only 0.142. Furthermore, according to the two-way interactions for all these coating parameters in Fig. 12(b), coating thickness all reflect greater interaction strength with mass and porosity, while coating porosity provides lower interaction strength with other parameters. These indicate that coating thickness and mass present the first and second order interactions for battery volumetric capacity case. These interpretable outputs are very useful as the obtained results are consistent with the experiences and conclusions from related experimental works, but this study demonstrates that how the proposed interpretable machine learning framework is able to explain the dynamic effects as well as interaction levels of coating parameters of interest, further helping engineers to obtain critical insights to understand the underlying complicated non-linear battery material and manufacturing behavior during battery manufacturing.

4.5. Comparisons and discussion

In this subsection, three case studies are designed to explore the hyperparameters searching of proposed RF regression models, the comparisons with other benchmarks and the illustration of importance
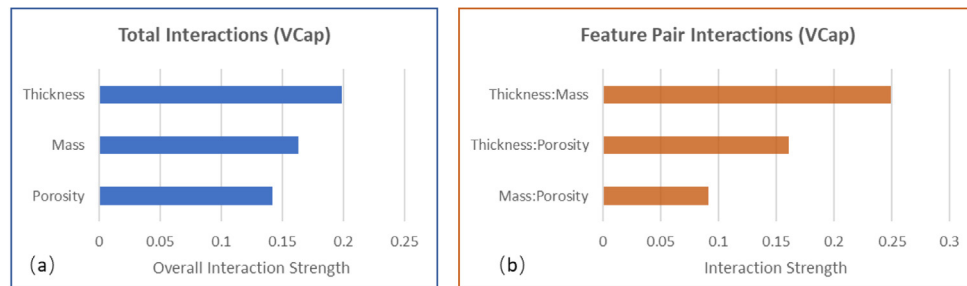
Fig. 12. Feature interactions for VCap case study. (a): Total interactions, (b): Feature pair interactions.

Table 3
Results of hyperparameter searching.

Hyperparameter search space	Cap (MCVA) [mAh]	GCap (MCVA) [mAh/g]	VCap (MCVA) [mAh/cm³]
$D = 60, n = 2$	0.049	1.618	18.323
$D = 80, n = 2$	0.042	1.507	17.278
$D = 100, n = 2$	**0.036**	1.412	**16.912**
$D = 120, n = 2$	0.036	**1.410**	16.920
$D = 140, n = 2$	0.038	1.433	16.916
$D = 60, n = 3$	0.051	1.617	18.572
$D = 80, n = 3$	0.044	1.532	17.231
$D = 100, n = 3$	0.039	1.441	17.013
$D = 120, n = 3$	0.040	1.438	17.002
$D = 140, n = 3$	0.040	1.440	16.989

Table 4
Performance indicators for VCap predictions through using different benchmarks.

Benchmarks	LR	SVM	AdaBoost model	Designed model
MAE [mAh/cm³]	41.323	31.029	17.013	16.912
RMSE [mAh/cm³]	11.742	7.535	4.812	4.820
R^2	0.71	0.88	0.98	0.98

ranking from RF, followed by the further discussion of battery manufacturing database creation and the motivation of regressor selection.

4.5.1. Hyperparameters searching

As mentioned in Section 3.4, two hyperparameters D and n are crucial to determine the performance of RF regression model. To perform a more thorough search, a randomized search strategy (Bergstra & Bengio, 2012) that sets up the random combination for model training and scores a classical performance indicator named the mean cross-validated accuracy (MCVA) is adopted here to determine the proper D and n for Cap, GCap and VCap prediction cases. To widen the domain of hyperparameters, the search space of D is set as: space(60,140,20), while the candidate of n is set as: [2,3], respectively. According to Table 3 that shows the prediction performance of all capacity types with different combinations of hyperparameters, it can be noted that both Cap and VCap obtain the best prediction results under the condition of $D = 100, n = 2$. Here the MCVAs for them are 0.036 [mAh] and 16.912 [mAh/cm³], respectively. For GCap case, the best result is achieved with the MCVA of 1.410 [mAh/g] under the condition of $D = 100, n = 3$, which is slightly 0.15% better than that of $D = 100, n = 2$. In this context, $D = 100, n = 2$ is able to provide the satisfactory prediction performance for all three capacity types of manufactured battery.

4.5.2. Comparisons with other benchmarks

To further investigate the effectiveness of the designed regression model, another three simple and state-of-the-art benchmarks including the linear regression (LR) model, the support vector machine (SVM)-based model and also the AdaBoost-based boosting model are utilized for comparison purpose. Specifically, LR model belongs to a linear method to fit the underlying mapping between input variables and a response. SVM is a kernel-based approach to transfer the inputs

into a high dimensional space for regression. AdaBoost-based boosting model is a classical boosting-based ensemble learning solution for regression (Liu, Peng, Li, & Chen, 2022). The VCap case is adopted as an illustration here as it achieves the worst prediction results from the designed RF model. Without the loss of generality, all these comparisons are carried out by using the Matlab 2021 statistics and machine learning toolbox with a 2.40 GHz Intel Pentium 4 CPU. Fig. 13 and Table 4 show the VCap prediction results and related performance indicators of all these methods after five folds cross-validation, respectively. It can be noted that LR model provides the worst prediction results as many observations are far away from the perfect prediction line. This further indicates that the underlying mapping between the coating parameters (mass, thickness, porosity) and the VCap presents a highly nonlinear relation. In contrast, through using the SVM model, the VCap prediction performance can be improved with a R^2 of 0.88, which is 23.9% larger than that of LR model. Here both the AdaBoost model and the designed RF model present good prediction results for VCap with 0.98 R^2, while the AdaBoost model achieves a slightly better RMSE value (0.17% decrease). Therefore, the designed RF model and AdaBoost-based boosting model are capable of presenting competent performance in the capacity prediction application of manufactured battery products.

4.5.3. Importance ranking from RF

It should be known that RF also has the capability to directly quantify the importance value of all input variables (Liu, et al., 2021). To reflect this type of input importance, the importance rankings of coating parameters from RF based on the aggregated Gini index are also given here. Fig. 14 illustrates the normalized importance weights of coating mass, thickness and porosity for all three battery capacity types obtained from RF models. It can be seen that although the normalized importance values between Cap and VCap are different, the trends of their importance rankings are the same for all three coating parameters. Obviously, coating thickness achieves the highest importance weight, indicating that this parameter is the most important one for the prediction of battery Cap and VCap. Here the coating mass and porosity present the second and third importance weights. For the GCap case, coating mass becomes the most important parameter, while the coating porosity still contributes the least to the prediction. This result is expected as the coating mass has strong and direct relations with the active material property, further significantly affecting the gravimetric capacity of the battery product. Furthermore, it can be noted that the quantified input importance from RF is a constant value, which is actually different from the interpretable results from ALE. Specifically, the former belongs to a type of statical importance, while the latter is able to reflect how the variation of input variables would dynamically affect the prediction results.

4.5.4. Discussion

(1) Database creation To build the data-driven model in real battery manufacturing applications, both the ways of creating own database and sharing data can work in different cases. From the experience, for the collaborated UK battery manufacturing industries
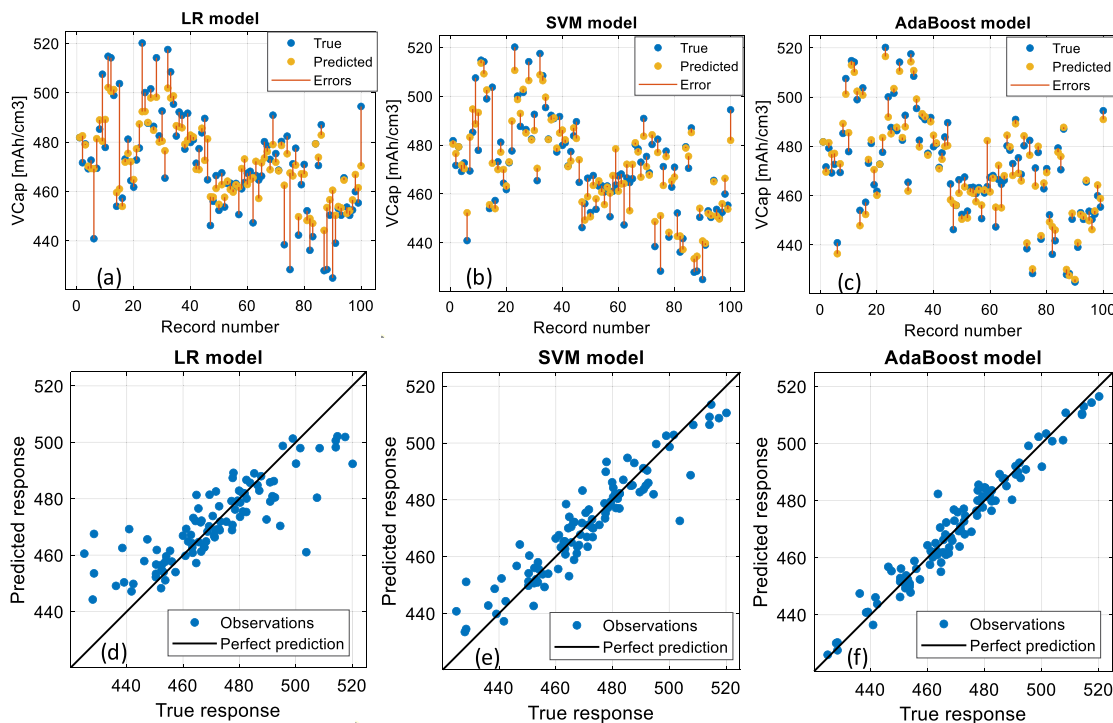
Fig. 13. VCap prediction results of different benchmarks. (a): LR model, (b): SVM model, (c): AdaBoost model, (d): Predicted versus actual plots for LR model, (e): Predicted versus actual plots for SVM model, (f): Predicted versus actual plots for AdaBoost model.
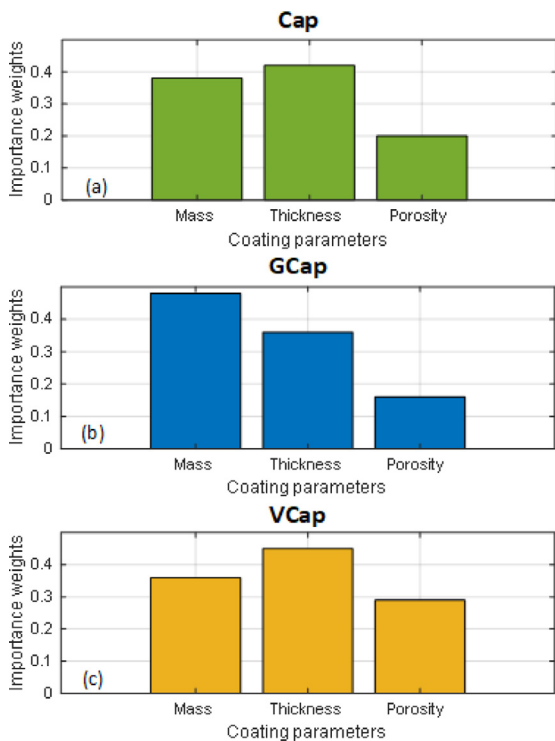

Fig. 14. Normalized importance weights for all three capacity types of battery products obtained from RF models. (a): Cap case, (b): GCap case, (c): VCap case.

such as UKBIC and Britishvolt, due to the sensitivity and confidentiality of manufacturing data, each manufacturer expects to create its own database. However, as supported in Aykol et al. (2020), in more academic research, the manufacturing databases are worth being shared through outsourcing battery manufacturing to central facilities

for constructing a more robust and generic model. Due to the superiority in terms of model interpretability and data-driven nature, the proposed machine learning framework could be conveniently extended to analyze other manufacturing databases, which has been proven by the stakeholders of the Nextrode project. On the other hand, to generate available battery manufacturing database with low costs, the 'design of experiments' solution, which defines the ranges of database by experts and ensures enough brake points are also given in between each of the control variables, is suggested (Niri, et al., 2022). It could make full use of battery manufacturing resources and significantly benefits the costs associated with the construction of battery manufacturing database for data-driven model development, which has been adopted by many UK battery manufacturers to generate modeling databases.

(2) Regressor selection For the selection of a deterministic regressor, different battery applications present different requirements and priorities for machine learning tools. For example, for the capacity degradation prediction in battery operation stage, as the uncertainty quantification around the predicted future time-series capacities is crucial for battery users to make reasonable decisions for avoiding unexpected operating failures and losses, the machine learning tools with the probabilistic forecast ability are highly required in this application (Liu, Shang, Ouyang, & Widanage, 2020; Liu, Tang, Teodorescu, Gao, & Meng, 2021). In contrast, for the battery manufacturing data analysis application, as battery manufacturing line contains a number of chemical, mechanical as well as electrical operations and would generate strongly-coupled parameters or variables that affect the performance of the manufactured battery, the interpretable machine learning tools to effectively analyze the manufacturing parameters and better quantify their interactions or effects during battery manufacturing are urgently required with higher priority.

5. Conclusion

Battery manufacturing plays a direct and pivotal role in determining the manufactured battery performance. However, it is difficult to analyze the strong-coupled parameters within a complicated

battery production chain and predict battery properties at the early-manufacturing stage. In this study, as suggested and highly required by UK battery manufacturers, an interpretable machine learning framework through combining the benefits of three effective and user-friendly AI tools is proposed to predict battery capacities and explain the dynamic effects as well as interactions of manufacturing parameters of interest. It should be noted that this is significantly important for battery manufacturers to better understand their manufacturing line and make reasonable battery property predictions at the early-manufacturing stage, which presents the recognized practical value to the corresponding industrial practitioners. Specifically, the framework is derived by integrating ALE and H-statistic with the RF-based regression model, which takes three key coating parameters (mass, thickness and porosity) as inputs to predict Cap, GCap and VCap of battery products, while their underlying parameter dynamical dependencies as well as interactions are also analyzed. The proposed framework is validated based on a reliable manufacturing dataset from a real battery manufacturing chain. Some conclusions can be made as: (1) After establishing RF-based regression models, all capacity types (Cap, GCap and VCap) of battery product can be accurately predicted with R^2 values over 0.98 by using coating mass, thickness and porosity as inputs at the early-stage production cases. (2) The ALE values of Cap, GCap and VCap all present a monotonically increasing relationship with the increase of coating mass, indicating that coating mass loading provides a positive effect on increasing all these three battery capacity types. (3) The interaction values of mass and thickness are always larger than porosity, implying that coating mass and thickness would provide more interactions with other parameters for all these three battery capacity prediction cases. To the best knowledge, this is the first known application that derives the interpretable RF-based regression framework to predict and analyze the dynamic effects of coating parameters on the properties of battery products. It makes the RF-based model become more interpretable and offers a convenient and smart alternative for parameter analyzes and product property predictions, especially in the cases of battery production chain where strong-coupled chemical, mechanical and electrical parameters are existed. This research also highlights the potential of interpretable machine learning to effectively predict and automatically obtain insights for the battery production chain. The future work would focus on the development of more interpretable machine learning tools for smarter control of battery manufacturing.

Declaration of competing interest

The authors declare that they have no known competing financial interests or personal relationships that could have appeared to influence the work reported in this paper.

Acknowledgments

References

Apley, D. W., & Zhu, J. (2020). Visualizing the effects of predictor variables in black box supervised learning models. *Journal of the Royal Statistical Society. Series B. Statistical Methodology*, *82*(4), 1059–1086.

Aykol, M., Herring, P., & Anapolsky, A. (2020). Machine learning for continuous innovation in battery technologies. *Nature Reviews Materials*, *5*(10), 725–727.

Bergstra, J., & Bengio, Y. (2012). Random search for hyper-parameter optimization. *Journal of Machine Learning Research*, *13*(2).

Biau, G., & Scornet, E. (2016). A random forest guided tour. *Test*, *25*(2), 197–227.

Cunha, R. P., Lombardo, T., Primo, E. N., & Franco, A. A. (2020). Artificial intelligence investigation of NMC cathode manufacturing parameters interdependencies. *Batteries & Supercaps*, *3*(1), 60–67.

Dey, S., Biron, Z. A., Tatipamula, S., Das, N., Mohon, S., Ayalew, B., et al. (2016). Model-based real-time thermal fault diagnosis of Lithium-ion batteries. *Control Engineering Practice*, *56*, 37–48.

Duffner, F., Kronemeyer, N., Tübke, J., Leker, J., Winter, M., & Schmuch, R. (2021). Post-lithium-ion battery cell production and its compatibility with lithium-ion cell production infrastructure. *Nature Energy*, *6*(2), 123–134.

Duquesnoy, M., Lombardo, T., Chouchane, M., Primo, E. N., & Franco, A. A. (2020). Data-driven assessment of electrode calendering process by combining experimental results, in silico mesostructures generation and machine learning. *Journal of Power Sources*, *480*, Article 229103.

Fang, H., Srivas, T., de Callafon, R. A., & Haile, M. A. (2017). Ensemble-based simultaneous input and state estimation for nonlinear dynamic systems with application to wildfire data assimilation. *Control Engineering Practice*, *63*, 104–115.

Feng, F., Hu, X., Liu, K., Che, Y., Lin, X., Jin, G., et al. (2020). A practical and comprehensive evaluation method for series-connected battery pack models. *IEEE Transactions on Transportation Electrification*, *6*(2), 391–416.

Feng, F., Hu, X., Liu, J., Lin, X., & Liu, B. (2019). A review of equalization strategies for series battery packs: variables, objectives, and algorithms. *Renewable and Sustainable Energy Reviews*, *116*, Article 109464.

Günther, T., Schreiner, D., Metkar, A., Meyer, C., Kwade, A., & Reinhart, G. (2020). Classification of calendering-induced electrode defects and their influence on subsequent processes of lithium-ion battery production. *Energy Technology*, *8*(2), Article 1900026.

Hoffmann, L., Grathwol, J. K., Haselrieder, W., Leithoff, R., Jansen, T., Dilger, K., et al. (2020). Capacity distribution of large lithium-ion battery pouch cells in context with pilot production processes. *Energy Technology*, *8*(2), Article 1900196.

Hu, X., Feng, F., Liu, K., Zhang, L., Xie, J., & Liu, B. (2019). State estimation for advanced battery management: Key challenges and future trends. *Renewable and Sustainable Energy Reviews*, *114*, Article 109334.

Hu, T., Ma, H., Liu, K., & Sun, H. (2022). Lithium-ion battery calendar health prognostics based on knowledge-data-driven attention. *IEEE Transactions on Industrial Electronics*.

Hu, T., Ma, H., Sun, H., & Liu, K. (2022). Electrochemical-theory-guided modelling of the conditional generative adversarial network for battery calendar ageing forecast. *IEEE Journal of Emerging and Selected Topics in Power Electronics*.

Hu, X., Zhang, K., Liu, K., Lin, X., Dey, S., & Onori, S. (2020). Advanced fault diagnosis for lithium-ion battery systems: A review of fault mechanisms, fault features, and diagnosis procedures. *IEEE Industrial Electronics Magazine*, *14*(3), 65–91.

Ju, F., Li, J., Xiao, G., Huang, N., & Biller, S. (2013). A quality flow model in battery manufacturing systems for electric vehicles. *IEEE Transactions on Automation Science and Engineering*, *11*(1), 230–244.

Kern, C. (2020). *Machine learning interpretation tools*. SAGE Publications Limited.

Klintberg, A., Zou, C., Fridholm, B., & Wik, T. (2019). Kalman filter for adaptive learning of two-dimensional look-up tables applied to OCV-curves for aged battery cells. *Control Engineering Practice*, *84*, 230–237.

Knoche, T., Surek, F., & Reinhart, G. (2016). A process model for the electrolyte filling of lithium-ion batteries. *Procedia CIRP*, *41*, 405–410.

Kwade, A., Haselrieder, W., Leithoff, R., Modlinger, A., Dietrich, F., & Droeder, K. (2018). Current status and challenges for automotive battery production technologies. *Nature Energy*, *3*(4), 290–300.

Li, Y., Liu, K., Foley, A. M., Zülke, A., Berecibar, M., Nanini-Maury, E., et al. (2019). Data-driven health estimation and lifetime prediction of lithium-ion batteries: A review. *Renewable and Sustainable Energy Reviews*, *113*, Article 109254.

Liaw, A., & Wiener, M. (2002). Classification and regression by randomforest. *R News*, *2*(3), 18–22.

Liu, K., Gao, Y., Li, K., Zhu, C., Fei, M., Peng, C., et al. (2022). Electrochemical modeling and parameterization towards control-oriented management of lithium-ion batteries. *Control Engineering Practice*.

Liu, K., Hu, X., Meng, J., Guerrero, J. M., & Teodorescu, R. (2021). Ruboost-based ensemble machine learning for electrode quality classification in Li-ion battery manufacturing. *IEEE/ASME Transactions on Mechatronics*.

Liu, K., Hu, X., Zhou, H., Tong, L., Widanage, W. D., & Marco, J. (2021). Feature analyses and modeling of lithium-ion battery manufacturing based on random forest classification. *IEEE/ASME Transactions on Mechatronics*, *26*(6), 2944–2955.

Liu, K., Li, K., & Zhang, C. (2017). Constrained generalized predictive control of battery charging process based on a coupled thermoelectric model. *Journal of Power Sources*, *347*, 145–158.

Liu, K., Peng, Q., Li, K., & Chen, T. (2022). Data-based interpretable modeling for property forecasting and sensitivity analysis of Li-ion battery electrode. *Automotive Innovation*, 1–13.

Liu, K., Peng, Q., Sun, H., Fei, M., Ma, H., & Hu, T. (2022). A transferred recurrent neural network for battery calendar health prognostics of energy-transportation systems. *IEEE Transactions on Industrial Informatics*.

Liu, K., Shang, Y., Ouyang, Q., & Widanage, W. D. (2020). A data-driven approach with uncertainty quantification for predicting future capacities and remaining useful life of lithium-ion battery. *IEEE Transactions on Industrial Electronics*, *68*(4), 3170–3180.

Liu, K., Tang, X., Teodorescu, R., Gao, F., & Meng, J. (2021). Future ageing trajectory prediction for Lithium-ion battery considering the knee point effect. *IEEE Transactions on Energy Conversion*.

Liu, K., Wang, Y., & Lai, X. (2022). *Data science-based full-lifespan management of lithium-ion battery: manufacturing, operation and reutilization*. Springer Nature.

Liu, K., Wei, Z., Zhang, C., Shang, Y., Teodorescu, R., & Han, Q. L. (2022). Towards long lifetime battery: AI-based manufacturing and management. *IEEE/CAA Journal of Automatica Sinica*.

Liu, K., Zou, C., Li, K., & Wik, T. (2018). Charging pattern optimization for lithium-ion batteries with an electrothermal-aging model. *IEEE Transactions on Industrial Informatics*, *14*(12), 5463–5474.

Loh, W. Y. (2011). Classification and regression trees. *Wiley Interdisciplinary Reviews: Data Mining and Knowledge Discovery*, *1*(1), 14–23.

Majdzik, P., Akielaszek-Witczak, A., Seybold, L., Stetter, R., & Mrugalska, B. (2016). A fault-tolerant approach to the control of a battery assembly system. *Control Engineering Practice, 55*, 139–148.

Mishra, C., & Subbarao, P. M. V. (2021). Design, development and testing a hybrid control model for RCCI engine using double Wiebe function and random forest machine learning. *Control Engineering Practice, 113*, Article 104857.

Molnar, C. (2020). *Interpretable machine learning*. Lulu.com.

Niri, M. F., Liu, K., Apachitei, G., Ramirez, L. R., Lain, M., Widanage, D., et al. (2021). Machine learning for optimised and clean Li-ion battery manufacturing: Revealing the dependency between electrode and cell characteristics. *Journal of Cleaner Production, 324*, Article 129272.

Niri, M. F., Liu, K., Apachitei, G., Román-Ramírez, L. A., Lain, M., Widanage, D., et al. (2022). Quantifying key factors for optimised manufacturing of Li-ion battery anode and cathode via artificial intelligence. *Energy and AI, 7*, Article 100129.

Ouyang, Q., Wang, Z., Liu, K., Xu, G., & Li, Y. (2019). Optimal charging control for lithium-ion battery packs: A distributed average tracking approach. *IEEE Transactions on Industrial Informatics*, *16*(5), 3430–3438.

Pourabdollah, M., Egardt, B., Murgovski, N., & Grauers, A. (2017). Effect of driving, charging, and pricing scenarios on optimal component sizing of a PHEV. *Control Engineering Practice, 61*, 217–228.

Reynolds, C. D., Slater, P. R., Hare, S. D., Simmons, M. J., & Kendrick, E. (2021). A review of metrology in lithium-ion electrode coating processes. *Materials & Design, 209*, Article 109971.

Schnell, J., Nentwich, C., Endres, F., Kollenda, A., Distel, F., Knoche, T., et al. (2019). Data mining in lithium-ion battery cell production. *Journal of Power Sources, 413*, 360–366.

Schünemann, J. H., Dreger, H., Bockholt, H., & Kwade, A. (2016). Smart electrode processing for battery cost reduction. *ECS Transactions*, *73*(1), 153.

Severson, K. A., Attia, P. M., Jin, N., Perkins, N., Jiang, B., Yang, Z., et al. (2019). Data-driven prediction of battery cycle life before capacity degradation. *Nature Energy*, *4*(5), 383–391.

Shafikhani, I. (2021). Energy management of hybrid electric vehicles with battery aging considerations: Wheel loader case study. *Control Engineering Practice, 110*, Article 104759.

Shang, Y., Liu, K., Cui, N., Wang, N., Li, K., & Zhang, C. (2019). A compact resonant switched-capacitor heater for lithium-ion battery self-heating at low temperatures. *IEEE Transactions on Power Electronics*, *35*(7), 7134–7144.

Tang, X., Gao, F., Liu, K., Liu, Q., & Foley, A. M. (2021). A balancing current ratio based state-of-health estimation solution for lithium-ion battery pack. *IEEE Transactions on Industrial Electronics*.

Tang, X., Liu, K., Wang, X., Gao, F., Macro, J., & Widanage, W. D. (2020). Model migration neural network for predicting battery aging trajectories. *IEEE Transactions on Transportation Electrification*, *6*(2), 363–374.

Turetskyy, A., Thiede, S., Thomitzek, M., von Drachenfels, N., Pape, T., & Herrmann, C. (2020). Toward data-driven applications in lithium-ion battery cell manufacturing. *Energy Technology*, *8*(2), Article 1900136.

Turetskyy, A., Wessel, J., Herrmann, C., & Thiede, S. (2021). Battery production design using multi-output machine learning models. *Energy Storage Materials*, *38*, 93–112.

Wang, Y., Tian, J., Sun, Z., Wang, L., Xu, R., Li, M., et al. (2020). A comprehensive review of battery modeling and state estimation approaches for advanced battery management systems. *Renewable and Sustainable Energy Reviews*, *131*, Article 110015.

Wanner, J., Weeber, M., Birke, K. P., & Sauer, A. (2019). Quality modelling in battery cell manufacturing using soft sensing and sensor fusion-a review. In *2019 9th international electric drives production conference* (pp. 1–9). IEEE.

Wei, Z., Zhao, J., Xiong, R., Dong, G., Pou, J., & Tseng, K. J. (2018). Online estimation of power capacity with noise effect attenuation for lithium-ion battery. *IEEE Transactions on Industrial Electronics*, *66*(7), 5724–5735.

Zhou, X., Stein, J. L., & Ersal, T. (2017). Battery state of health monitoring by estimation of the number of cyclable Li-ions. *Control Engineering Practice, 66*, 51–63.